
[View Journal Online](#)
[View Article Online](#)

Virtual molecular docking study of some novel carboxamide series as new anti-tubercular agents

Mustapha Abdullahi ^{1,*}, Adamu Uzairu ¹, Gideon Adamu Shallangwa ¹,
 David Ebuka Arthur ², Bello Abdullahi Umar ¹ and Muhammad Tukur Ibrahim ¹

¹ Department of Chemistry, Faculty of Physical Sciences, Ahmadu Bello University, 810107, Zaria, Nigeria
mustychem19@gmail.com (M.A.), adamuuzairu@yahoo.com (A.U.), gashallangwa@gmail.com (G.A.S.), abdallahbum@yahoo.com (B.A.U.),
muhdtk1988@gmail.com (M.T.I.)

² Department of Chemistry, Baze University, 900108, Abuja, Nigeria
davidebukaaarthur@gmail.com (D.E.A.)

* Corresponding author at: Department of Chemistry, Faculty of Physical Sciences, Ahmadu Bello University, 810107, Zaria, Nigeria.
 e-mail: mustychem19@gmail.com (M. Abdullahi).

RESEARCH ARTICLE



 10.5155/eurjchem.11.1.30-36.1955

Received: 27 December 2020

Received in revised form: 25 January 2020

Accepted: 27 January 2020

Published online: 31 March 2020

Printed: 31 March 2020

KEYWORDS

Protein
 PLANTS
 Docking
 MolDock
 Binding affinity
 Scoring functions

ABSTRACT

A virtual docking simulation study was performed on thirty-five newly discovered compounds of *N*-(2-phenoxy) ethyl imidazo[1,2-*a*] pyridine-3-carboxamide (IPA), to explore their theoretical binding energy and pose with the active sites of the *Mycobacterium tuberculosis* target (DNA gyrase). The chemical structures of the compounds were drawn correctly with ChemDraw Ultra software, and then geometrically optimized at DFT level of theory with Spartan 14 software package. Consequently, the docking analysis was carried out using Molegro Virtual Docker (MVD). Five complexes (Complex 5, 24, 25, 33 and 35) with high binding energy were selected to examine their binding pose with the active sites of the protein. The docking results suggested a good MolDock score (≥ -90 kcal/mol) and Protein-Ligand ANT System (PLANTS) score (≥ -60 kcal/mol) which depicted that the compounds can efficiently bind with the active sites of the target. However, compound 5 has the best binding pose with the MolDock score of -140.476 kcal/mol which formed three hydrogen bond interactions with the Gln 538, Ala 531, and Ala 533 amino acid residues. This research gives a firsthand theoretical knowledge to improve the binding efficiency of these compounds with the target.

Cite this: *Eur. J. Chem.* 2020, 11(1), 30-36

Journal website: www.eurjchem.com

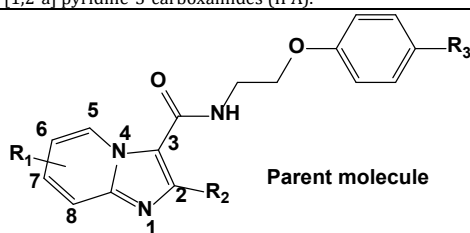
1. Introduction

Tuberculosis (TB) is one of the world's most deadly respiratory bacterial diseases caused by *Mycobacterium tuberculosis* (MTB). It was amongst the top ten deadliest diseases caused by a single infectious agent [1]. Recently, the number of patients getting life-saving treatment for TB in 2018 has enormously augmented due to increased detection and diagnosis [2].

Nigeria is ranked among the top seven nations that account for 64% of the total danger of tuberculosis worldwide [3]. It has been reported in the global tuberculosis report of the World Health Organization (2019) which showed the statistics of over 202 countries and territories that account for more than 99% of the world's population and estimated a high number of TB cases.

The occurrence of extensively drug-resistant (XDR) and the progression of multidrug-resistant (MDR) TB have attracted the attention of medicinal chemists who are in search of novel inhibitors with improved bioactivities.

Literature has shown that imidazo[1,2-*a*]pyridine-3-carboxamide (IPA) as an anti-tubercular candidate is currently in the second phase of clinical trials, and it was reported to have resilient inhibitory potency or anti-mycobacterial activity [4]. *Mycobacterium tuberculosis* DNA gyrase is the only type II topoisomerase that replicates the DNA using ATP energy. It is made up of GyrA subunits where the DNA binding domain is located and GyrB subunits which are responsible for ATP activity. However, Gyr A or Gry B can be blocked by these inhibitors for the termination of the DNA replication or to prevent their binding to the DNA [5]. The concept of computational chemistry like computer-aided drug design (CADD) might save the time of discovering or designing new compounds with better potency, and also reduce the cost of synthesis [6]. Virtual docking simulation is very important when carrying out a structure-based drug design (SBDD). Molecular docking simulation predicts the binding affinity as well as the binding pose of the ligand with the active sites of a target (receptor).

Table 1. Substitution arrangement of the imidazo [1,2-a] pyridine-3-carboxamides (IPA).

Compound	R ₁	R ₂	R ₃	Mw (g/mol)
1	6-NO ₂	Me	Br	419.03
2	6-F	Me	Br	392.04
3	6-Cl	Me	Br	408.01
4	6-Br	Me	Br	451.96
5	6-OMe	Me	Br	404.06
6	7-Me	Me	Br	388.06
7	7-Cl	Me	Br	408.01
8	8-Me	Me	Br	388.06
9	8-Cl	Me	Br	408.01
10	5-Cl	Me	Br	408.01
11	6-Cl	Et	Br	422.02
12	6-F	Et	Br	406.05
13	6-Br	Et	Br	465.97
14	7-Cl	Et	Br	422.02
15	8-Cl	Et	Br	422.02
16	6-Me	Et	Br	402.08
17	6-Me	n-Pr	Br	416.09
18	6-Me	c-Pr	Br	414.08
19	6-F	n-Pr	Br	420.07
20	6-F	c-Pr	Br	418.05
21	6-Cl	n-Pr	Br	436.04
22	6-Cl	c-Pr	Br	434.02
23	7-Cl	c-Pr	Br	434.02
24	7-Me	c-Pr	Br	414.08
25	6-Me	n-Pr	Cl	372.14
26	6-F	Me	Cl	348.09
27	7-Cl	Et	Cl	378.07
28	6-Cl	Et	Cl	378.07
29	6-Cl	n-Pr	Cl	392.09
30	6-F	n-Pr	Cl	376.12
31	7-Cl	c-Pr	Cl	390.07
32	6-Cl	Et	OMe	374.12
33	6-Me	c-Pr	OMe	366.18
34	6-Me	Et	OMe	354.18
35	6-Br	Et		522.20

The ultimate aim and objective of the present study were to perform *in-silico* docking analysis of some newly synthesized IPA compounds as a potent anti-tubercular agent using Molegro Virtual Docker.

2. Experimental

2.1. Computer hardware and software

Dell computer system, with processor properties of Intel® Core i3-6100U CPU Dual@2.30GHz, 12 GB (RAM) was used to carry out this computational study. The software packages installed include Chemdraw Ultra software V. 12.0.2 [7], Spartan'14 V 1.1.2 [8] developed by Wavefunction Inc., Molegro Virtual Docker [9] and Discovery Studio Visualizer V. 16.1 [10].

2.2. Virtual docking method

2.2.1. Equilibrium geometry of ligands and protein structure

Thirty-five compounds were selected from the newly discovered and synthesized series of *N*-(2-phenoxy) ethyl imidazo[1,2-a] pyridine-3-carboxamide (IPA) as anti-tubercular agents [11]. The chemical structure of the compounds were drawn using ChemDraw Ultralevel software

V12.0.2 (Table 1), then geometrically optimized using Spartan 14 software at ground state with Density Functional Theory (DFT/B3LYP/6-31G** [12-15] in a vacuum which is finally saved as Protein Data Bank (PDB) file format [16]. The crystal structure of the *Mycobacterium tuberculosis* DNA Gyrase was downloaded from the protein data bank website <http://www.rcsb.org> with PDB code: 3IG0, at 2.1 Å resolution of the model quality from X-ray diffraction method [17].

2.2.2. Virtual docking study

The docking simulation in this study was carried out using Molegro Virtual Docker (MVD) software version 2013.6.0 [18] developed by the CLC-bio Company. At first, before the docking process begins, the protein structure and the optimized ligands were appropriately prepared. All structural errors in the amino acid residue of the protein were checked and repaired [19]. Consequently, bonds, bond orders, hybridization, charges (calculated by MVD) were assigned to the models (protein and ligands). In addition, explicit hydrogens were created, and flexible torsions in ligands were detected.

2.2.3. Docking parameters

M. tuberculosis DNA Gyrase has 185 amino acid residues on the terminal chain of the protein which is a small protein. Hence, the docking radius was set on 18 Å so as to cover the

entire surface of the detected cavities in the binding sites. MolDock scoring function at 0.30 Å grid resolutions was selected for the docking process. The choice of MolDock is based on the fact that it is a fast and accurate scoring function [20,21]. Subsequently, an alternative scoring function termed as PLANTS score was also used to recheck and generate the binding scores of the complexes formed. MolDock operation in MVD software employed piecewise linear potential (PLP) scoring function, it takes charges and directionality of hydrogen bonding into consideration. The docking scoring function is defined as;

$$E_{\text{score}} = E_{\text{intra}} + E_{\text{inter}} \quad (1)$$

where E_{intra} is the internal energy of the ligand which computed as,

$$E_{\text{intra}} = \sum_{i \in \text{ligand}} \sum_{j \in \text{ligand}} E_{\text{PLP}}(r_{ij}) + \sum_{\text{flexible bonds}} A[1 - \cos(m\theta - \theta_0)] + E_{\text{Clash}} \quad (2)$$

The twofold summation in the expression is between all-atom pairs in the ligand with the exception of those atom pairs which are connected with less than two bonds. The second term is a torsional energy contribution from the torsional motion of the atoms, parameterized based on the types of hybridization of the bonded atoms, and θ represents the torsional angle. The third term which is E_{clash} contributes a penalty of 1000 as long as the distance between two heavy atoms is not greater than 2.0 Å. By implication, E_{clash} term corrects ligand conformation that is infeasible. The E_{inter} describes the ligand-protein residual interaction energy, defined as;

$$E_{\text{inter}} = \sum_{i \in \text{ligand}} \sum_{j \in \text{ligand}} \left[E_{\text{PLP}}(r_{ij}) + 332.0 \frac{q_i q_j}{4r_{ij}^2} \right] \quad (3)$$

where the summation covers all heavy atoms in the active ligand and protein together with any existing cofactors, and displaceable water molecules if present. The second term is the contribution from the electrostatic interactions among charged atoms, which is a coulombic potential with an inverse related square root of distance between two atoms apart. While the numerical score of 332.0 in the expression is a constant which converts the units of the electrostatic energy to kcal/mol.

Protein-Ligand ANT System (PLANTS) scoring function is defined by:

$$E_{\text{plantscore}} = f_{\text{PLP}} + f_{\text{clash}} + f_{\text{tors}} + f_{\text{csite}} - 20 \quad (4)$$

where the first terms are the PLP potential, and it is similar to the parametrized PLP potential in the MolDock scoring function. However, PLP potential in PLANTS scores considered more interaction types including nonpolar, repulsive, hydrogen bonding and so on. f_{tors} and f_{clash} are torsional potentials for the flexible bonds and internal ligand clashes respectively [19]. The f_{csite} term depicts a penalty computed provided that a pose (ligand conformation) is situated outside the binding site. While the -20 is energy constant for the Protein-Ligand ANT System (PLANTS) docking search algorithm. The MolDock Simplex Evolution (MolDock SE) docking algorithm search was also employed [9], which runs 10 times for each ligand with 1500 iterations and population size of 50 [22]. Furthermore, the docking operation converged after 1500 iterations with the least minimized energy of poses [23]. The most stable complexes from the docking results were exported to Discovery Studio so as to visualize major residual interactions of the ligands with the active sites of the protein.

3. Results and discussions

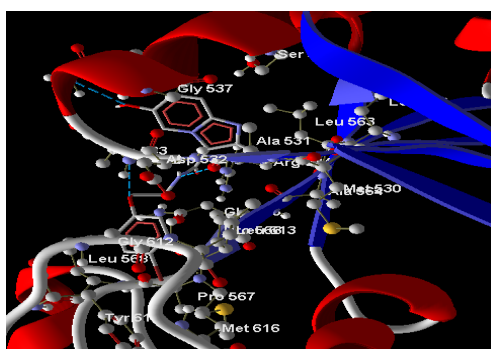
Virtual docking simulation is an optimization process, where the sole objective is to explore the most stable ligand binding pose with a target (receptor). The technique encompasses sampling the 3D- coordinate space of the binding site in the target and computing the binding affinity of each possible orientation of the ligand within the active sites which form the complex. As such, the highest binding score corresponds to the most stable complex. Molecular docking results in this study were generated using Molegro Virtual Docker V. 6.0 [23] as stated earlier. Table 2 shows docking energy and the re-rank score of each scoring function for the best pose in the ligand-target complex. The binding scores of the complexes range from -103 to -140 kcal/mol based on the MolDock score, and PLANTS scores range from -63 to 78 kcal/mol. Thus, compound 5, 24, 25, 33, and 35 were selected as the best inhibitors when they lock with the target (MTB - DNA Gyrase) due to their higher binding scores from both MolDock and PLANTS scoring functions. However, the entire 35 compounds have MolDock score greater than -90 kcal/mol which indicates that the inhibitors can bind target efficiently.

Compound 5 has the highest H-bond energy of -5.144 kcal/mol which formed three major H-bond interactions with different amino acid residues, wherewith -NH interact with Ala 531 at distance of 2.1 Å, oxygen of bromobenzene moiety interact with Ala 533 (1.91 Å), and oxygen from -OCH₃ attached to benzene ring from the imidazo[1,2-a] pyridine formed H-bond interaction with Gln 538 at bond distance of 2.31 Å. Also, the bromobenzene moiety formed five hydrophobic interactions with Pro 566, Leu 613, Met 616, Met 616, and Try 610 at different bond distances of 4.04, 5.11, 5.15, 3.69, and 3.87 Å, respectively, while the imidazo[1,2-a] pyridine forms four hydrophobic interactions with only two amino acid residues of Ala 533 and Ala 531. The major interaction types of compound 5 with the binding pockets of the target are visualized using the Discovery Studio and Molegro Virtual Viewer respectively as shown in Figure 1a-c.

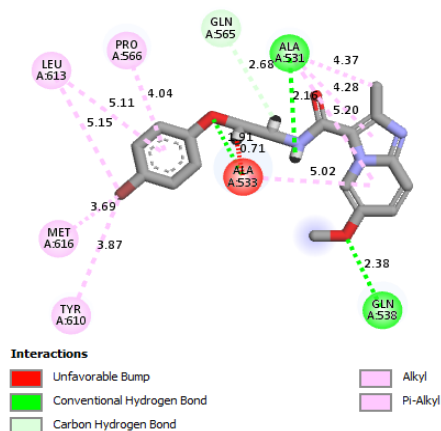
Compound 24 with H-bond energy of -1.6102 kcal/mol formed two major H-bond interactions, in which the oxygen of carbonyl (-CO) attached to imidazo[1,2-a] pyridine interact with two different amino acids (Ala 533 and Asp 534) at bond distances of 3.34 and 3.96 Å, respectively. The 2-cyclopropyl-6-methylimidazo[1,2-a]pyridine moiety in compound 24 formed eight hydrophobic interaction with Leu 613, Met 616, Pro 566, Ala 531, Leu 568, Arg 609 residues, and bromobenzene moiety forms only one hydrophobic interaction with Val 535 at a distance of 4.77 Å. Compound 25 has no H-bond but formed eight hydrophobic interactions in which 6-methyl-2-propylimidazo[1,2-a]pyridine moiety of the inhibitor interact with Met 616, Leu 568, Try 610, Leu 613, Ala 533, Pro 566 amino acid residues at different bond distances, and chlorobenzene moiety of the compound formed five hydrophobic interaction with Leu 563, Leu 529, Ala 531. Compound 33 binds with H-bond energy of -2.83173 kcal/mol, where oxygen of carbonyl in 2-cyclopropyl-6-methylimidazo[1,2-a] pyridine moiety interact with Pro 566 residue, and -NH group interact with Ala 533 resulting to two major H-bond interactions at different distances, while three hydrophobic interactions were formed with Leu 568, Pro 566, and Ala 533 amino acid. Compound 35 also formed two major H-bond interactions with Ala 564 and Arg 634 having H-bond energy of -1.3371 kcal/mol, and nine hydrophobic interactions with different amino acid residues at different bond distances respectively. The 2D and 3D binding poses of complex 24, 25, 33 and 35 were accordingly shown in Figure 2a-c, 3a-c, 4a-c, and 5a-c, while other interactions including electrostatic and steric interactions of the complexes were also shown in Table 3.

Table 2. Binding score of the inhibitors to *M. tuberculosis* DNA Gyrase based on MolDock, PLANTs scoring function and Reranking score.

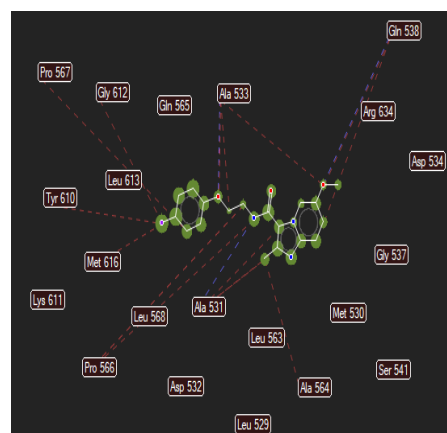
Complex	E _{intra} (kcal/mol)	E _{inter} (kcal/mol)	MolDock score (kcal/mol)	Plants score (kcal/mol)	Rerank score	Heavy atoms
1	14.633	-135.410	-120.778	-63.5814	-85.0878	26
2	17.730	-121.693	-103.964	-67.6286	-85.7196	24
3	11.714	-125.648	-113.934	-66.0500	-83.6646	24
4	-0.0096	-121.217	-121.269	-65.3775	-79.7315	24
5	6.724	-147.199	-140.476	-64.9392	-91.1801	25
6	16.791	-113.492	-113.493	-70.2678	-88.0665	24
7	17.270	128.789	-111.520	-71.7892	-89.0645	24
8	17.997	-124.631	-106.632	-68.9545	-88.8032	24
9	9.595	-116.183	-106.587	-70.5702	-85.6460	24
10	8.516	-111.535	-103.020	-69.9792	-69.6327	24
11	13.192	-123.692	-110.502	-73.5411	-89.1749	25
12	8.665	-116.146	-107.481	-68.9313	-85.5038	25
13	20.960	-135.934	-114.958	-67.3621	-67.7593	25
14	14.593	-133.117	-118.524	-74.9269	-95.6256	25
15	15.154	-127.155	-112.002	-69.6234	-89.5573	25
16	12.878	-125.672	-112.795	-69.6465	-88.9493	25
17	14.054	-121.969	-107.915	-70.5942	-88.7408	26
18	13.454	125.145	-111.691	-70.6211	-88.6235	26
19	9.572	-127.421	-117.849	-68.5039	-96.5660	26
20	4.354	-122.293	-107.939	-73.6718	-88.1530	26
21	18.522	-129.591	-111.068	-71.9622	-83.0864	26
22	20.385	-122.184	-101.799	-71.6454	-86.3710	26
23	14.609	136.021	-121.411	-78.4866	-96.5763	26
24	14.977	-139.309	-124.332	-78.3878	-101.047	26
25	9.975	-143.064	-133.089	-68.8083	-81.5543	26
26	13.782	-123.351	-109.568	-69.8936	-89.8933	24
27	21.114	-129.713	-108.599	-69.3726	-85.4175	24
28	18.027	-129.559	-111.532	-70.2911	-91.8876	25
29	12.196	-125.406	-113.210	-74.5718	-90.8904	26
30	12.410	-129.957	-117.546	-73.3149	-92.4200	26
31	11.136	-126.062	-114.925	-75.1457	-92.6054	26
32	17.216	-137.370	-120.153	-69.1705	-93.6688	26
33	10.340	-138.840	-128.500	-70.5756	-105.393	27
34	9.590	-130.952	-121.362	-71.2562	-94.0835	26
35	20.772	-138.297	-117.523	-75.8123	-92.5562	37



(a) Docked view of compound 5 with the active site of the target 3IG0.

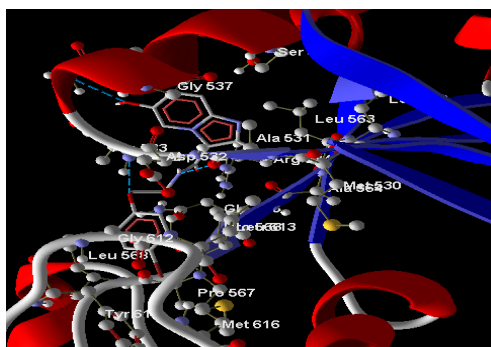


(b) Hydrogen bond (Green) and hydrophobic interactions of compound 5 with the active site of target 3IG0 from Discovery Studio Viewer.

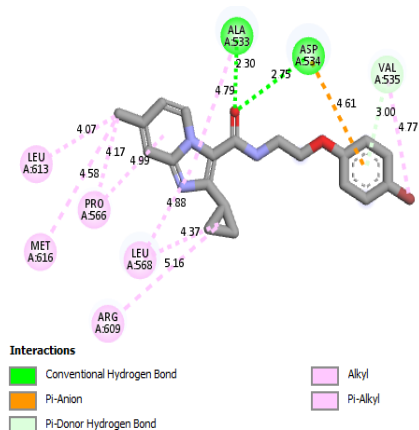


(c) Hydrogen bond (Blue lines) and steric interactions (brown lines) of compound 5 with the active site of target 3IG0 from Molegro Virtual Viewer.

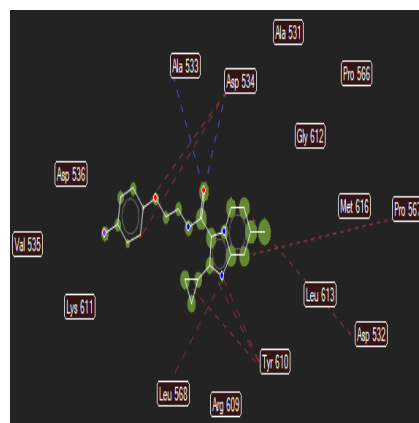
Figure 1. 3D and 2D binding pose of complex 5.



(a) Docked view of compound 24 with the active site of the target 31G0.

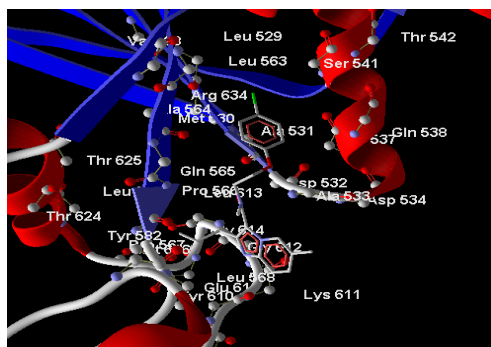


(b) Hydrogen bond (Green) and hydrophobic interactions of compound 24 with the active site of target 31G0 from Discovery Studio Viewer.

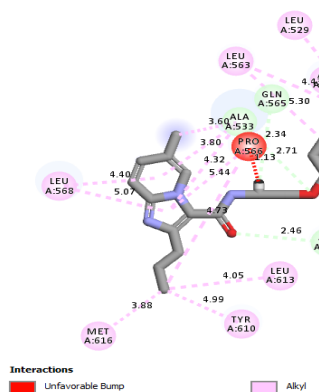


(c) Hydrogen bond (Blue lines) and steric interactions (brown lines) of compound 24 with the active site of target 31G0 from Molegro Virtual Viewer.

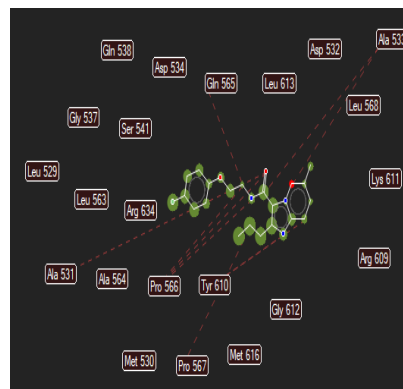
Figure 2. 3D and 2D Binding pose in complex 24.



(a) Docked view of compound 25 with the active site of the target 31G0.



(b) Hydrogen bond (Green) and hydrophobic interactions of compound 25 with the active site of target 31G0 from Discovery Studio Viewer.



(c) Hydrogen bond (Blue lines) and steric interactions (brown lines) of compound 25 with the active site of target 31G0 from Molegro Virtual Viewer.

Figure 3. 3D and 2D Binding pose in complex 25.

Table 3. Residual interactions of the best pose.

Complex	H-Bond energy (kcal/mol)	H-Bond interactions	Hydrophobic interactions	Other interactions (Steric and electrostatic)
5	-5.144	Gln 538, Ala 531, Ala 533	Pro 566, Leu 613, Met 616, Try 610, Ala 533, Ala 531	Arg 634, Ala 533, Ala 564, Ala 531, Ala 533, Pro 566, Met 616, Try 610, Pro 567, Gly 612
24	-1.6102	Ala 533, Asp 534	Leu 613, Met 616, Pro 566, Leu 568, Arg 609, Val 535	Pro 567, Asp 532, Try 610, Leu 568, Asp 534
25	0	-	Met 616, Leu 568, Try 610, Leu 613, Ala 533, Pro 566, Leu 563, Leu 529, Ala 531	Ala 531, Pro 566, Pro 567, Try 610, Ala 533, Gln 565
33	-2.83173	Pro 566, Ala 533	Leu 568, Pro 566, Ala 533	Arg 634, Lys 611, Ala 531, Pro 567, Ala 564, Asp 532
35	-1.3371	Ala 564, Arg 634	Ala 643, Leu 647, Ala 531, Pro 566, Ala 533	Gln 565, Ala 564, Pro 566, Ala 531, Ala 533, Leu 647, Ala 643, Ser 541

4. Conclusion

The virtual docking simulation approach employed theoretically confirmed the potency of the compounds with the MTB-DNA gyrase as the molecular target. The MolDock which is a fast and more accurate scoring function was used followed by PLANTS scoring function so as to increase the accuracy of the docking operation. The docking results revealed a good MolDock score (≥ -90 kcal/mol) and PLANTS score (≥ -60 kcal/mol) which depicted that the ligands can bind with the active site of the target efficiently. However, the outcomes of this research theoretically revealed the lead compounds, and provide a direction when carrying out an in-silico structure-based drug design for exploring more potent hypothetical compounds.

Acknowledgments

The authors expressed their profound gratitude to members of staff in The Physical Chemistry Unit, Department of Chemistry, Ahmadu Bello University Zaria for their technical assistance.

Disclosure statement

Conflict of interests: The authors declare that they have no conflict of interest.

Author contributions: All authors contributed equally to this work.

Ethical approval: All ethical guidelines have been adhered.

Sample availability: Samples of the compounds are available from the author.

ORCID

Mustapha Abdullahi

 <http://orcid.org/0000-0002-8533-6245>

Adamu Uzairu

 <http://orcid.org/0000-0002-6973-6361>

Gideon Adamu Shallangwa

 <http://orcid.org/0000-0002-0700-9898>

David Ebuka Arthur

 <http://orcid.org/0000-0001-8564-868X>

Bello Abdullahi Umar

 <http://orcid.org/0000-0003-0984-5969>

Muhammad Tukur Ibrahim

 <http://orcid.org/0000-0002-6146-5667>

References

- Zhai, W.; Wu, F.; Zhang, Y.; Fu, Y.; Liu, Z. *Int. J. Mol. Sci.* **2019**, *20*, 340, 1-18.
- Mabhula, A.; Singh, V. *Med. Chem. Comm.* **2019**, *10*, 1342-1360.
- Ogbuabor, D. C.; Onwujekwe, O. E. *Inf. Dis. Pov.* **2019**, *8*, 1-11.
- Zhaoyang, W.; Yu, L.; Linhu, L.; Rui, Z.; Bin, W.; Kai, L.; Mingliang, L.; Xuefu, Y. *ACS Med. Chem. Lett.* **2016**, *7*(12), 1130-1133.
- Lanez, T.; Lanez, E. *Int. J. Pharmacol. Phytochem. Ethnomed.* **2016**, *2*, 5-12.
- Abdullahi, M.; Uzairu, A.; Shallangwa, G. A.; Mamza, P.; Arthur, D. E.; Ibrahim, M. T. *J. King Saudi Uni. Sci.* **2019**, *32*(1), 770-779.
- Cousins, K. R. *J. Am. Chem. Soc.* **2005**, *127*(11), 4115-4116.
- Shao, Y.; Molnar, L. F.; Jung, Y.; Kussmann, J.; Ochsenfeld, C.; Brown, S. T.; Gilbert, A. T. B.; Slipchenko, L. V.; Levchenko, S. V.; O'Neill, D. P.; DiStasio, R. A.; Lochan, R. C.; Wang, T.; Beran, G. J. O.; Besley, N. A.; Herbert, J. M.; Lin, C. Y.; Van Voorhis, T.; Chien, S. H.; Sodt, A.; Steele, R. P.; Rassolov, V. A.; Maslen, P. E.; Korambath, P. P.; Adamson, R. D.; Austin, B.; Baker, J.; Byrd, E. F. C.; Dachsels, H.; Doerksen, R. J.; Dreuw, A.; Dunietz, B. D.; Dutoi, A. D.; Furlani, T. R.; Gwaltney, S. R.; Heyden, A.; Hirata, S.; Hsu, C. P.; Kedziora, G.; Khalliulin, R. Z.; Klunzinger, P.; Lee, A. M.; Lee, M. S.; Liang, W.; Lotan, I.; Nair, N.; Peters, B.; Proynov, E. I.; Pieniazek, P. A.; Rhee, Y. M.; Ritchie, J.; Rosta, E.; Sherrill, C. D.; Simmonett, A. C.; Subotnik, J. E.; Woodcock, H. L.; Zhang, W.; ell, A. T.; Chakraborty, A. K.; Chipman, D. M.; Keil, F. J.; Warshel, A.; Hehre, W. J.; Schaefer, H. F.; Kong, J.; Krylov, A. I.; Gill, P. M. W.; Head-Gordon, M. (Spartan, Wavefunction Inc., Irvine, CA, USA). *Phys. Chem. Chem. Phys.* **2006**, *8*, 3172-3191.
- Thomsen, R.; Christensen, M. H. *J. Med. Chem.* **2006**, *49*(11), 3315-3321.
- Biovia, D. S. CA, USA: San Diego, Discovery studio visualizer, 2017.
- Wang, A.; Lv, K.; Li, L.; Liu, H.; Tao, Z.; Wang, B.; Liu, M.; Ma, C.; Ma, X.; Han, B.; Wang, A.; Lu, Y. *Eur. J. Med. Chem.* **2019**, *178*, 715-725.
- Abdullahi, M.; Shallangwa, G. A.; Ali, T.; Uzairu, A. *J. Eng. Exact. Sci.* **2019**, *5*(1), 63-78.
- Becke, A. D. *J. Chem. Phys.* **1993**, *98*, 5648-5652.
- Lee, C.; Yang, W.; Parr, R. G. *Phys. Rev. B* **1988**, *37*, 785-789.
- Mustapha, A.; Shallangwa, G.; Ibrahim, M. T.; Bello, A. U.; Ebuka, D. A.; Uzairu, A.; Mamza, P. *J. Turk. Chem. Soc. Chem.* **2018**, *5*(3), 1387-1398.
- Murtaza, S.; Altaf, A. A.; Hamayun, M.; Iftikhar, K.; Tahir, M. N.; Tariq, J.; Faiz, K. *Eur. J. Chem.* **2019**, *10*(4), 358-366.
- Piton, J.; Petrella, S.; Delarue, M.; Andre-Leroux, G.; Jarlier, V.; Aubry, A.; Mayer, C. *PLoS ONE* **2010**, *5*(8), e12245.
- Kusumaningrum, S.; Budianto, E.; Kosela, S.; Sumaryono, W.; Juniarti, F. *J. App. Phar. Sci.* **2014**, *4*(11), 47-53.
- Yadav, M.; Khandelwal, R.; Urvy, M.; Srinitha, S.; Khandekar, N.; Nayarriseri, A.; Sugunakar, V.; Sanjeev, K. S. *Asian Pac. J. Cancer Prev.* **2019**, *20*(9), 2681-2692.
- Torktaz, I.; Mohamadhashem, F.; Esmaeili, A.; Behjati, M.; Sharifzadeh, S. *Bioimpacts.* **2013**, *3*(3), 141-144.
- Mishra, V.; Kashyap, S.; Hasija, Y. *J. Taibah Univ. Sci.* **2015**, *9*(1), 20-26.
- Madhuri, M.; Prasad, C.; Avupati, V. R. *Int. J. Comp. Appl.* **2014**, *95*(6), 13-16.
- Giacoppo, J. O. S.; Franca, T. C. C.; Kuca, K.; Cunha, E. F. F.; Abagyan, R.; Mancini, D. T.; Ramalho, T. C. *J. Biom. Struc. Dyn.* **2015**, *33*(9), 2048-2058.



Copyright © 2020 by Authors. This work is published and licensed by Atlanta Publishing House LLC, Atlanta, GA, USA. The full terms of this license are available at <http://www.eurjchem.com/index.php/eurjchem/pages/view/terms> and incorporate the Creative Commons Attribution-NonCommercial (CC BY NC) (International, v4.0) License (<http://creativecommons.org/licenses/by-nc/4.0>). By accessing the work, you hereby accept the Terms. This is an open access article distributed under the terms and conditions of the CC BY NC License, which permits unrestricted non-commercial use, distribution, and reproduction in any medium, provided the original work is properly cited without any further permission from Atlanta Publishing House LLC (European Journal of Chemistry). No use, distribution or reproduction is permitted which does not comply with these terms. Permissions for commercial use of this work beyond the scope of the License (<http://www.eurjchem.com/index.php/eurjchem/pages/view/terms>) are administered by Atlanta Publishing House LLC (European Journal of Chemistry).